UC Berkeley
UC Berkeley Previously Published Works

Title

Experimental determination of hydrogen isotopic equilibrium in the system H2O(l)-H2(g) from 3 to 90 °C

Permalink

https://escholarship.org/uc/item/95x7v4jp

Authors

Hochscheid, Flora
Turner, Andrew C
Lotem, Noam
et al.

Publication Date

2025-04-01

DOI

10.1016/j.gca.2025.02.029

Peer reviewed

eScholarship.org
Powered by the California Digital Library
University of California

Geochimica et Cosmochimica Acta 394 (2025) 368–382

Contents lists available at ScienceDirect

Geochimica et Cosmochimica Acta

journal homepage: www.elsevier.com/locate/gca

Experimental determination of hydrogen isotopic equilibrium in the system $H_2O_{(l)}$-$H_{2(g)}$ from 3 to 90 °C

Flora Hochscheid[a,*], Andrew C. Turner[a,b], Noam Lotem[c], Markus Bill[d], Daniel A. Stolper[a,d]

[a] Department of Earth and Planetary Science, University of California, Berkeley, CA 94720, USA
[b] Current address: U.S. Geological Survey, Central Energy Resources Science Center, Denver, CO 80225, USA
[c] Division of Geological and Planetary Sciences, California Institute of Technology, Pasadena, CA 91107, USA
[d] Energy Geosciences Division, Lawrence Berkeley National Laboratory, 1 Cyclotron Road, Berkeley, CA 94720, USA

ARTICLE INFO

Associate editor: Shuhei Ono

Keywords:
Hydrogen stable isotopes
Hydrogen isotopic equilibrium
Experimental calibration

ABSTRACT

Molecular hydrogen (H_2) is found in a variety of settings on and in the Earth from low-temperature sediments to hydrothermal vents, and is actively being considered as an energy resource for the transition to a green energy future. The hydrogen isotopic composition of H_2, given as D/H ratios or δD, varies in nature by hundreds of per mil from ~−800 ‰ in hydrothermal and sedimentary systems to ~+450 ‰ in the stratosphere. This range reflects a variety of processes, including kinetic isotope effects associated with formation and destruction and equilibration with water, the latter proceeding at fast (order year) timescales at low temperatures (<100 °C). At isotopic equilibrium, the D/H fractionation factor between liquid water and hydrogen (${}^{D}\alpha_{H2O(l)\text{-}H2(g)}$) is a function of temperature and can thus be used as a geothermometer for H_2 formation or re-equilibration temperatures. Multiple studies have produced theoretical calculations for hydrogen isotopic equilibrium between H_2 and water vapor. However, only three published experimental calibrations used in geochemistry exist for the H_2O-H_2 system: two between 51 and 742 °C for $H_2O_{(g)}$-$H_{2(g)}$ (Suess, 1949; Cerrai et al., 1954), and one in the $H_2O_{(l)}$-$H_{2(g)}$ system for temperatures <100 °C (Rolston et al., 1976). Despite these calibrations existing, there is uncertainty on their accuracy at low temperatures (<100 °C; e.g., Horibe and Craig, 1995).

Here we present a new experimental calibration of the equilibrium hydrogen isotopic fractionation factor for liquid water and molecular hydrogen from 3 to 90 °C. Equilibration was achieved using platinum catalysts and verified via experimental bracketing by approaching final values of ${}^{D}\alpha_{H2O(l)\text{-}H2(g)}$ at a given temperature from both higher (top-bracket) and lower (bottom-bracket) initial ${}^{D}\alpha$ values. Our calibration yields the following equation:

$$1000\times\ln{}^{D}\alpha_{H2O(l)-H2(g)} = -526.48 + \frac{559{,}316}{T}$$

Where T is in Kelvin. We find that our calibrations differ from prior experimental calibrations by, on average, up to 20 ‰ and prior theoretical results by up to, on average, 25 ‰. Good agreement with theoretical results (<11 ‰ differences) is found for calculations that consider both anharmonic effects and the Diagonal Born-Oppenheimer correction.

1. Introduction

Molecular hydrogen (H_2) occurs in numerous environments on and in the Earth from low-temperature sediments to hydrothermal vents (e.g., Charlou et al., 2002; Lin et al., 2005; Sherwood Lollar et al., 2014; Milkov, 2022; Pester et al., 2018). It forms in the subsurface and reacts through the action of microbial metabolisms, via water–rock reactions (e.g., serpentinization), and from radiolysis of water (e.g., Zgonnik, 2020). Beyond its role in many subsurface reactions, H_2 has recently been identified as a potential energy resource that can extracted from subsurface deposits (e.g., Prinzhofer et al., 2018, 2019; Truche et al., 2024) or generated from renewably produced energy sources and potentially stored underground for later use (Lord, 2009; Lord et al., 2014; Tarkowski, 2019; Zivar et al., 2021; Aftab et al., 2022; Amirthan

---

[*] Corresponding author.
E-mail address: fhochscheid@berkeley.edu (F. Hochscheid).

https://doi.org/10.1016/j.gca.2025.02.029
Received 18 September 2024; Accepted 25 February 2025
Available online 28 February 2025
0016-7037/© 2025 Elsevier Ltd. All rights are reserved, including those for text and data mining, AI training, and similar technologies.

and Perera, 2023; Taiwo et al., 2024).

Important to the study of environmental H_2 is ascertaining the conditions (e.g., temperature) and chemical pathways of formation and any later reactions during transport and storage. One way these can be constrained is based on the bulk (or average) stable isotopic composition of H_2, given by its D/H ratio. This ratio is expressed using δD notation where $\delta D_{sample} = ([D/H]_{sample}/[D/H]_{standard} - 1) \times 1000$ (given in per mil) and where the standard is VSMOW. H_2 displays a large isotopic range in nature, from ∼−800 ‰ to −300 ‰ in sediments and seafloor hydrothermal systems (e.g., Proskurowski et al., 2006; Sherwood Lollar et al., 2007; Telling et al., 2018) to +440 ‰ in the stratosphere (e.g., Rahn et al., 2003).

In sediments and hydrothermal systems it is generally assumed that H_2 is in hydrogen isotopic equilibrium with local waters such that the δD of H_2 (δD_{H2}) is set by δD of local waters ($\delta D_{H2O(l)}$) and temperature of the system. This assumption is supported by the observation of rapid obtainment (weeks to years) of isotopic equilibration in experiments between H_2 and liquid water at <100 °C (e.g., Pester et al., 2018).

Temperature plays a role as it sets the equilibrium distribution of D/H between H_2 and H_2O, which is described by the hydrogen isotopic fractionation factor (${}^{D}\alpha_{H2O(l)\text{-}H2(g)}$) between $H_2O_{(l)}$ and $H_{2(g)}$:

$$ {}^{D}\alpha_{H2O(l)-H2(g)} = \frac{\left[\frac{D}{H}\right]_{H2O(l)}}{\left[\frac{D}{H}\right]_{H2(g)}} = \frac{\delta D_{H2O(l)} + 1000}{\delta D_{H2(g)} + 1000} \tag{1} $$

The temperature dependence of ${}^{D}\alpha_{H2O(l)\text{-}H2(g)}$ has been measured experimentally and calculated theoretically over the past 90 years in multiple studies, but there still exists disagreement on the precise temperature dependence at low (<100 °C) temperatures. Here we create such a calibration experimentally using modern techniques and standardization at low temperatures (<100 °C). Before discussing this, we first provide a brief introduction to prior determinations of the temperature dependence of ${}^{D}\alpha_{H2O(l)\text{-}H2(g)}$ in order to both provide the basis for the motivation of this study and place it into the context of past efforts.

Experimental and theoretical studies of the equilibrium hydrogen isotopic composition of $H_{2(g)}$ and water vapor $H_2O_{(v)}$ (i.e., ${}^{D}\alpha_{H2O(v)\text{-}H2(g)}$) were carried out within a few years of the discovery of deuterium (1931) and followed by additional studies through the 1940 s associated with the Manhattan Project (see Kirshenbaum et al. (1951). Though of historical importance, these results (theoretical and experimental) are not in general usage.

The only experimental determination of ${}^{D}\alpha_{H2O(l)\text{-}H2(g)}$ used in isotope geochemistry in which $H_2O_{(l)}$ and $H_{2(g)}$ were directly equilibrated is from Rolston et al. (1976). Equilibration was done from 6 to 95 °C using a catalytic Pt-impregnated Teflon sheet and deuterium enriched waters (∼2.0 and ∼3.5 mol % D vs. ∼0.015 % in nature). Isotopic compositions were determined by mass spectrometry via peak-hopping where H_2 and HD ion beams were measured separately. In contrast, modern mass spectrometric methods measure ion beams simultaneously on multiple collectors. H_2 measurements were standardized using isotopically enriched waters converted to H_2 over hot uranium. The isotopic compositions of waters were determined gravimetrically by diluting D_2O (99.8 %) with unenriched waters. This differs from modern approaches in which community standards with agreed upon D/H ratios are used for standardization. We raise these details as inaccuracy in measured D/H ratios of H_2O or H_2, if they are not sufficiently well correlated with a slope of 1 for the different sample types (H_2 vs. H_2O), will lead to inaccurate measures of ${}^{D}\alpha_{H2O(l)\text{-}H2(g)}$.

Despite being the only direct experimental determination of ${}^{D}\alpha_{H2O(l)\text{-}H2(g)}$, the calibration of Rolston et al. (1976) is not in general usage. One possibility for this is based on an assessment by Horibe and Craig (1995) who stated that a fit to the Rolston et al. (1976) data (${}^{D}\alpha_{H2O(l)\text{-}H2(g)}$ vs. 1/T) yielded a standard deviation too large (±45 ‰) to be useful for geochemical applications.

Calibrations of ${}^{D}\alpha_{H2O(l)\text{-}H2(g)}$ have also been determined indirectly by combining experimental calibrations between $H_{2(g)}$ and water vapor (${}^{D}\alpha_{H2O(v)\text{-}H2(g)}$) with those for liquid water and water vapor (${}^{D}\alpha_{H2O(l)\text{-}H2O(v)}$) (e.g., Pester et al., 2018; Wang et al., 2018; Mangenot et al., 2023). The two calibrations used for ${}^{D}\alpha_{H2O(v)\text{-}H2(g)}$ are from Suess (1949) and Cerrai et al. (1954). Today these experimental values are generally converted to ${}^{D}\alpha_{H2O(l)\text{-}H2(g)}$ using the calibration for ${}^{D}\alpha_{H2O(l)\text{-}H2O(g)}$ from Horita and Wesolowski (1994). We examine each of these in turn.

Suess (1949) experimentally equilibrated H_2 gas with water vapor from 80 to 200 °C using Pt-catalysts and deuterium enriched waters (4 to 60 mol % D). H_2 was converted to water and the deuterium content measured by pycnometry (i.e., by density). Cerrai et al. (1954) equilibrated H_2 gas with water vapor from 51–742 °C using a Pt-catalyst supported on either charcoal or silica gel and with isotopically enriched water (2.5 mol % D). They cite Kirshenbaum et al. (1951) to describe their isotopic methodology wherein H_2 is converted to H_2O and deuterium contents determined by measuring the index of refraction of water (which is sensitive to D content). Importantly, the work of Cerrai et al. (1954) and Suess (1949), both in terms of standardization and measurement, are not those used today for D/H determinations of H_2 or H_2O.

An alternative to using experimental calibrations is to instead employ theoretical calculations. To our knowledge, direct calculations of ${}^{D}\alpha_{H2O(l)\text{-}H2(g)}$ do not exist, presumably due to the difficulty of treating water as a liquid in theoretical calculations. Instead, theoretical calculations of ${}^{D}\alpha_{H2O(g)\text{-}H2(g)}$ (i.e., all gas phase molecules) can be combined with experimental determinations of ${}^{D}\alpha_{H2O(l)\text{-}H2O(g)}$ to create an estimate of ${}^{D}\alpha_{H2O(l)\text{-}H2(g)}$. We are aware of five theoretical estimations of ${}^{D}\alpha_{H2O(g)\text{-}H2(g)}$ done using modern approaches: Bottinga (1968), Bardo and Wolfsberg (1976), Richet et al. (1977), Gropp et al. (2021), and Turner et al. (2021). These postdate the initial papers from Urey (1947) and Bigeleisen and Mayer (1947) that established the common methodology for doing such calculations. In detail, these studies differ in approach. For example, Gropp et al. (2021) performed calculations following the harmonic approximations of Urey (1947) and Bigeleisen and Mayer (1947). Bottinga (1968), Bardo and Wolfsberg (1976), and Richet et al. (1977) incorporated anharmonic effects via secondary corrections to harmonic calculations. Turner et al. (2021) included anharmonicity using a path integral approach. Additionally, Bardo and Wolfsberg (1976) and Turner et al. (2021) incorporated a correction for the Born-Oppenheimer approximation (termed the Diagonal Born-Oppenheimer Correction, or DBOC).

In Fig. 1A we summarize these results with a compilation of ${}^{D}\alpha_{H2O(l)\text{-}H2(g)}$ from 0 to 374 °C (freezing to critical point of pure water). Studies that determined values of ${}^{D}\alpha_{H2O(g)\text{-}H2(g)}$ (i.e. all except Rolston et al. (1976)) are converted to ${}^{D}\alpha_{H2O(l)\text{-}H2(g)}$ using values of ${}^{D}\alpha_{H2O(l)\text{-}H2O(g)}$ from Horita and Wesolowksi (1994). The large range of ${}^{D}\alpha_{H2O(l)\text{-}H2(g)}$ over this temperature range (∼1100 ‰) makes it difficult to see differences between studies. We address this in Fig. 1B by displaying the deviation in ${}^{D}\alpha_{H2O(l)\text{-}H2O(g)}$ relative to the study of Turner et al. (2021). We use this study as our reference as it uses both high-level approaches to calculate partition function ratios that include anharmonicity and uses high-accuracy potential energies. We observe a total range of about ±60 ‰ relative to the reference curve, with typical differences around ±25 ‰.

A strong motivation for the work presented here is that there is currently no agreement on which calibration to use in a given study. Some recent studies have used prior experimental calibrations such as Wang et al. (2015) who used the calibration of Cerrai et al. (1954) and Mangenot et al. (2023) who used the calibration from Suess (1949). However most prior work we have examined employed theoretical calculations of ${}^{D}\alpha_{H2(g)\text{-}H2O(g)}$ from Bardo and Wolfsberg (1976) combined with a calibration of ${}^{D}\alpha_{H2O(l)\text{-}H2O(g)}$. This usage likely stems from the study of Horibe and Craig (1995) that provides an equation for ${}^{D}\alpha_{H2O(l)\text{-}H2(g)}$ (their equation 8) that is based on the combination of ${}^{D}\alpha_{H2O(v)\text{-}H2}$

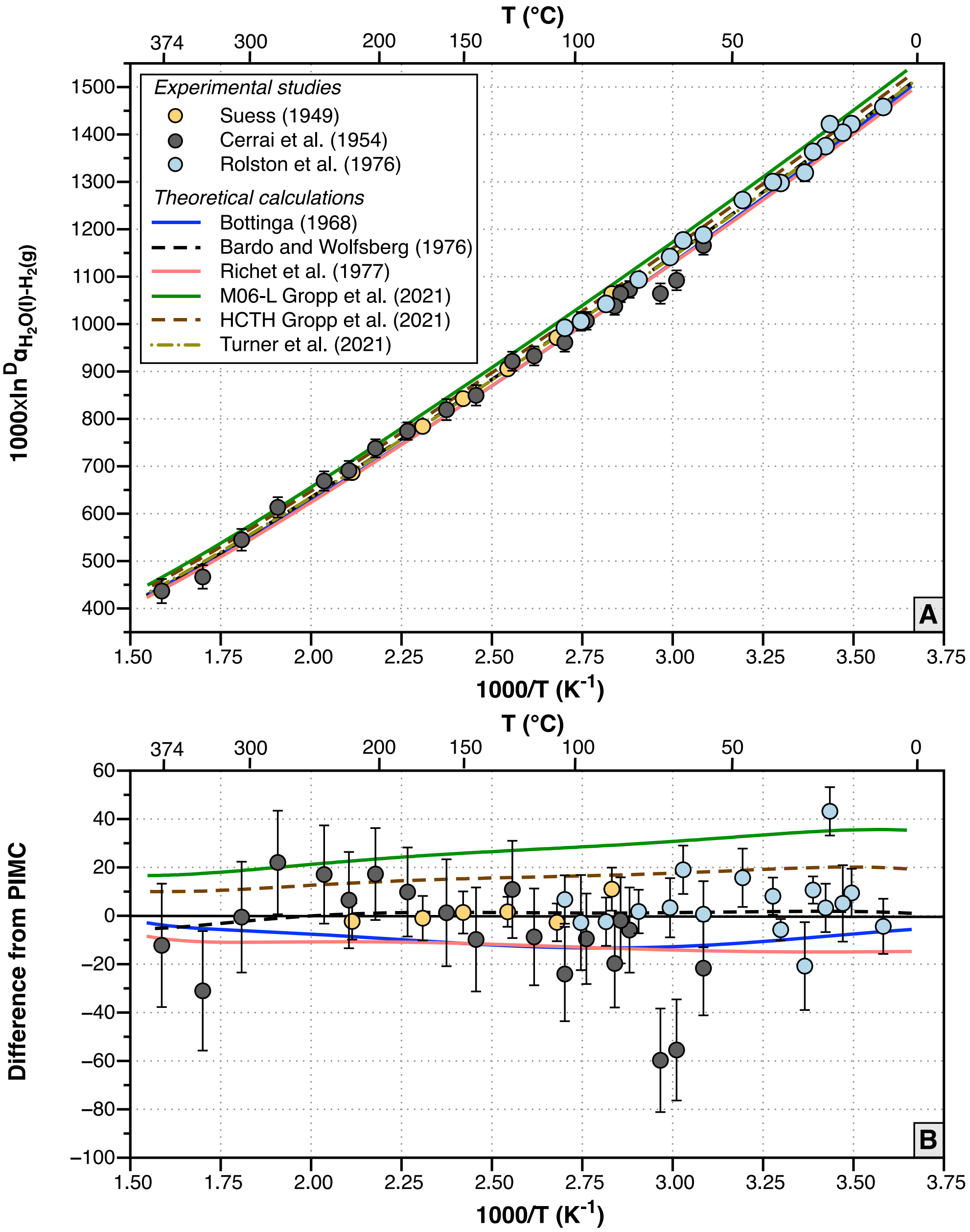

Fig. 1. A) Previous experimental and theoretical calculations of 1000 × $\ln^{D}\alpha_{H2O(l)\text{-}H2(g)}$ versus 1000/T (K^{-1}). B) Difference of 1000 × $\ln^{D}\alpha_{H2O(l)\text{-}H2(g)}$ values from experimental and theoretical calculations minus the theoretical fit from Turner et al. (2021). Error bars for data from Suess (1949), Cerrai et al. (1954) and Rolston et al. (1976) are ±1σ as reported in the original study. Data from Suess (1949), Cerrai et al. (1954), and the theoretical studies are given in the studies as $^{D}\alpha_{H2O(v)\text{-}H2(g)}$. We converted them to $^{D}\alpha_{H2O(l)\text{-}H2(g)}$ using the calibration for $^{D}\alpha_{H2O(l)\text{-}H2O(g)}$ from Horita and Wesolowski (1994). We only interpolate best-fit lines over the range of either the theoretical or experimental data from which they were derived.

$_{(g)}$ from Bardo and Wolfsberg (1976) and $^{D}\alpha_{H2O(l)\text{-}H2O(g)}$ of Horita and Wesolowski (1994) (e.g., Proskurowski et al., 2006; Bradley et al., 2010; Kawagucci et al., 2010; Foustoukos et al., 2012; Suda et al., 2014; Etiope et al., 2017; Pester et al., 2018; Ricci et al., 2022).

As it stands, we consider it unclear which, if any, of these prior calibrations (theoretical or experimental) is the best to use. The choice matters given deviations of up to around ±60 ‰ (Fig. 1B) between studies. Such deviations lead to ~10 °C differences in estimated temperatures from 0–100 °C and up to 35 °C up to the critical point of water. With the renewed interest in studying molecular H_2 due to its increasing importance as an energy resource, we consider it important to resolve these issues. To this end, we present a direct calibration $^{D}\alpha_{H2O(l)\text{-}H2(g)}$ from 3 to 90 °C using modern stable isotopic techniques.

2. Materials and methods

2.1. Experimental setup and sampling

We isotopically equilibrated liquid water and molecular hydrogen using platinum catalysts over a temperature range of 3 to 90 °C. We employed two different platinum catalysts: catalytic rods used for H_2/H_2O equilibration in Thermo Scientific Gas Bench systems (Thermo Fisher Scientific no. 1091831) and pellets of platinum on alumina (Pt-Al; Sigma Aldrich 232114-25G). We note that Pt-based catalysts have been used for decades to promote $H_2O_{(l)}$-$H_{2(g)}$ and $H_2O_{(g)}$-$H_{2(g)}$ hydrogen isotope equilibration (e.g., Suess, 1949; Kirshenbaum et al., 1951; Cerrai et al., 1954; Rolston et al., 1976; Horita, 1988; Ohba and Hirabayashi, 1996).

Experiments were carried out by placing either one Pt-catalyst rod or ~2 g of Pt-Al pellets inside a 20 mL Wheaton glass vial (Fig. 2). We sealed the vial with a crimped blue chlorobutyl stopper and pumped away atmospheric gas using a vacuum line (to a baseline pressure of 10–20 mTorr). We next added water to the vials. For experiments using Pt-catalyst rods, ~8 mL of water at room temperature (~20 °C) and pressure were injected into the vial with a syringe such that the water level was at the approximate mid-point of the Pt surface on the catalytic rod (Fig. 2A). For experiments with Pt-Al pellets, ~1.5 mL of water (at room temperature and pressure) was added such that some of the pellets were above the fill line (Fig. 2B).

Vials were then again exposed to vacuum for ~15 min to remove any air added in this process. We verified that this step did not alter the isotopic composition of the water beyond uncertainty (see Appendix Table S1 for additional details). Finally, ~21 mL (at room temperature and pressure) of H_2 (99.999 %, δD_{H2} = –235 ‰) were injected into the 20 mL vial, pressurizing the head space above atmospheric pressure.

Vials were sampled by removing 0.3 mL of gas with a gas-tight syringe and injecting the sample into a 6 mL Wheaton glass vial pre-sealed with a crimped blue chlorobutyl stopper and pre-purged with helium (99.9 %). Finally, samples were stored at room temperature until later mass spectrometric analysis. Such analyses always took place within 8 days of sampling (Appendix Table S2). We verified that isotopic compositions of H_2 do not change during storage via replicate isotopic measurements as a function of storage time (see Appendix A.1 of Supplementary Material for more details).

Most (41/46) experiments employed milli-Q water (18.2 MΩ/cm H_2O) that was taken from a 1L glass bottle filled at the beginning of the study, sealed when not in use with parafilm, and sub-sampled as needed. In other experiments (5/46), we created waters with higher δD_{H2O} by adding deuterium enriched water (99.9 % D_2O) to milli-Q water and stored as above.

We tested and verified that both Pt-rods and Pt-Al catalysts yield the same values for $^{D}\alpha_{H2O(l)-H2O(g)}$ by conducting experiments with both catalysts (but in separate vials) with the same initial water composition and at the same temperature (specifically 15, 20, 25, 30, 35, 60 and 70 °C).

2.2. Bracketing experiments

Equilibration experiments were conducted following a bracketing methodology (O'Neil, 1986) in which equilibrium isotopic compositions are approached from two different directions. Specifically, initial δD_{H2} and δD_{H2O} values were chosen or experimentally set such they created initial $^{D}\alpha_{H2O(l)-H2(g)}$ values higher (top bracket) or lower (bottom bracket) than the final equilibrium $^{D}\alpha_{H2O(l)-H2(g)}$ value. In this approach, experimentally determined $^{D}\alpha_{H2O(l)-H2(g)}$ values can be considered successfully bracketed and thus represent the equilibrium compositions when both top and bottom bracketing experiments yield the same $^{D}\alpha_{H2O(l)-H2(g)}$ value (within some nominal uncertainty) at a given experimental temperature.

For our experiments, all vials started as bottom-brackets because the initial δD of the hydrogen (δD_{H2} = –235 ‰) and waters (δD_{H2O} = −94.6 ‰ and +349.0 ‰) result in values of $^{D}\alpha_{H2O(l)-H2(g)}$ = 1.184 and 1.763, both of which are significantly less than all prior theoretical and experimentally derived values for $^{D}\alpha_{H2O(l)-H2(g)}$ (~4.5 to 2.7) over the 3–90 °C studied temperature range.

We created top brackets by pre-equilibrating vials at lower temperatures than the final desired temperature (either 3 or 10 °C depending on the final temperature). Based on prior work, $^{D}\alpha_{H2O(l)-H2(g)}$ is expected to monotonically decrease with increasing temperature (e.g., Rolston et al., 1976; Horibe and Craig, 1995; Turner et al., 2021) such that an initial exposure to and equilibration at colder temperatures will create $^{D}\alpha_{H2O(l)-H2(g)}$ higher than expected final values once the vial is heated to final experimental temperatures. For completeness, we also verified that all top brackets started with higher-than-final $^{D}\alpha_{H2O(l)-H2(g)}$ values. We did this by sampling an aliquot of gas prior to heating the experiment to the final desired temperature and analyzing its isotopic composition.

2.3. Temperatures of experiments

Experiments were conducted at 3, 10, 15, 20, 22, 25, 30, 35, 40, 50, 60, 70, and 90 °C (given as round numbers — precise temperatures are given in Appendix Table S2 and used in all calculations and figures). For the 10 and 15 °C experiments, top brackets were created by pre-equilibrating at 3 °C. For all other temperatures, pre-equilibration was done at 10 °C. Experiments at 3, 10, 15 and 20 °C were conducted in recirculating cooling baths (Thermo Neslab RTE-111 and Cole-Parmer AD 7LR-20) with digital temperature set points. The top bracket experiments at 20, 25, 30, 40, 70 °C and the bottom bracket experiments at 22, 25, 30, 35, 40, 70 °C were conducted in three non-recirculating water baths (Cole Parmer StableTemp, models GH-14576–04 5L and WB-400 2L) with digital temperature set points. In all water bath systems, vials were fully immersed in the water. During sampling, vials were removed from the bath, exposing them to air temperature for ~2 min.

For top bracket experiments at 35, 50, 60 and 90 °C and bottom bracket experiments at 50, 60 and 90 °C, we used a dry-block heater with a digital temperature controller (VMR no. 75838–270). These heaters have 8 pre-drilled positions for vials. The vials are taller than the pre-drilled holes such that the top of vials where the septum is located are exposed to room temperature during the experiment. In order to limit the temperature gradient across the vial we placed an identical aluminum block over the one being heated, covering the vials. This

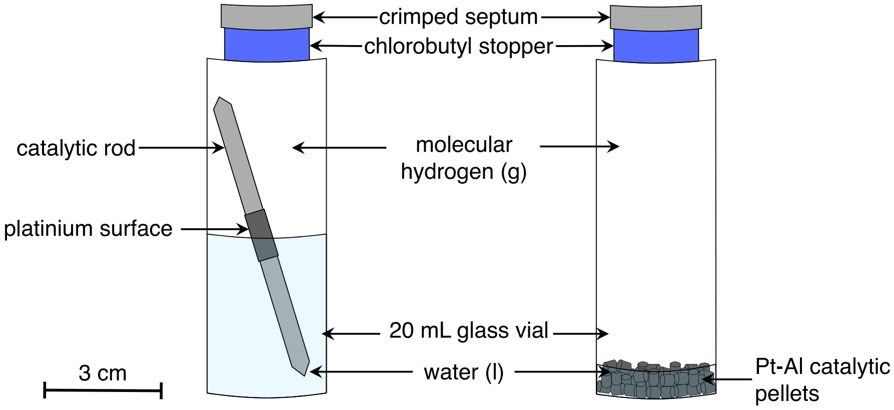

Fig. 2. Schematic of the experimental setups used in the hydrogen-water isotope equilibration experiments. On the left: platinum catalytic rods. On the right: platinum-on-alumina pellets.

limited the vertical gradient in the heated block to <0.5 °C.

The temperature reported for every experiment is based on the temperature measured using an external Type K Chromed/Alumel thermocouple (the same for all experiments). We observed good agreement (<0.2 °C) between the temperature measured in water baths and heating blocks with the external thermocouple vs. that given by the digital readout. This thermocouple yields accurate temperatures (<0.5 °C deviation) for boiling water. Temperatures were observed to vary by ≤0.2 °C in the water baths and within ±0.5 °C in the dry-block heaters. These temperatures variations are equivalent to approximately ±1 to ±3 ‰ in expected values of 1000 × $\ln^{D}\alpha_{H2O(l)\text{-}H2(g)}$ respectively.

2.4. Isotopic measurements

The isotopic composition of $H_{2(g)}$ was analyzed at the Center for Isotope Geochemistry in the Lawrence Berkeley National Laboratory (LBNL) using a gas-chromatograph (GC) Thermo Scientific GC Trace Gas Ultra system instrument connected to a Thermo Scientific Delta V Plus Isotope Ratio Mass Spectrometer (IRMS). The H_2 was separated via chromatography on an HP-mole sieve fused silica capillary column (30 m x 0.32 mm) using helium as carrier gas. After GC separation, any traces of water were removed with a liquid nitrogen trap and then the hydrogen isotope ratio of the H_2 was measured in the IRMS. Samples were measured in three different analytical sessions (October 2023, November 2023, January-February 2024).

Measured δD_{H2} were first corrected for instrument linearity as described by Turner et al. (2021). To limit the size of the linearity correction, we injected samples such that peak areas for the mass 2 ion beam were between 30 and 70 Vs. Following the linearity correction, δD values were placed onto the VSMOW-SLAP scale using three calibrated H_2 gas standards from Oztech Trading Corp. ($\delta D_{H2\ (VSMOW)}$ = –762.6, −364.1 and −124.8 ‰). All individual measurements of standards are given in Appendix Table S3. To check for accuracy, we also measured three other calibrated H_2 gas standards with declared values from ATG ($\delta D_{H2\ (VSMOW)}$ = –758.7, −362.8 and −123.6 ‰) at both the Center for Isotope Geochemistry (Lawrence Berkeley National Laboratory (LBNL)) as well as using a 253 Ultra high-resolution gas source isotope ratio mass spectrometer (Thermo Scientific 253) in the Division of Geological and Planetary Sciences at Caltech following the method described by Mangenot et al. (2023).

The isotopic composition of $H_2O_{(l)}$ was measured using a Los Gatos Research (LGR) liquid water analyzer IWA-35-EP instrument at the Center for Isotope Geochemistry (LBNL). The measurements were standardized against at least three LGR standards that had a range of δD_{H2O} that spanned the sample range (i.e., corrections for samples were always interpolations of standards). Different standards were used in different measurement sessions depending on the range of expected values of water samples. See Appendix Table S4 for additional information. To verify the accuracy of measurements, several USGS standards (USGS49, USGS47, W43152, and USGS48 with $\delta D_{H2\ (VSMOW)}$ = –396.5, −151.1, −110.3, and −1.8 ‰ respectively) were also analyzed in the June 2024 session (Appendix Table S4) and they were all within 2.8 ‰ of expected values. The δD of liquid water was measured before the experiments as well as after some experiments where Pt-catalyst rods were used (water could not be extracted from experiments using Pt-Al pellets; see Appendix Table S1).

2.5. Accounting for changes in δD_{H2O} following equilibration

Based on the experimental conditions used, the exchange of hydrogen isotopes between $H_{2(g)}$ and $H_2O_{(l)}$ will result in an increase in δD_{H2O}. One way to correct for this would be to measure the δD_{H2O} of samples following equilibration. However, we could not do this for experiments using pellets as we could not extract the water. Instead, we calculated the final δD_{H2O} for each experiment using a mass balance approach where:

$$n_{H_2i} \times \delta D_{H_2i} + n_{H_2Oi} \times \delta D_{H_2Oi} = n_{H_2f} \times \delta D_{H_2f} + n_{H_2Of} \times \delta D_{H_2Of} \tag{2}$$

In equation (2), *n* is the number of moles of hydrogen at the initial (*i*) or final equilibrium (*f*) point.

The values for *n* for H_2O and H_2 are known based on the volumes injected. For molecular hydrogen, samples are always at 1 atm prior to injection and we assume a room temperature of 22 °C to calculate the number of moles. We assume *n* does not change for H_2 or H_2O over the experiment (i.e., $n_i = n_f$). The δD of the initial water, initial molecular hydrogen, and final molecular hydrogen are all known allowing us to solve for the final δD_{H2O} value. This correction results in changes from initial to final values of ~1 ‰ for catalytic rods (unreacted milli-Q water −94.6 ‰ vs. corrected values = –93.6 ‰) and ~5 ‰ for pellets (corrected value = –89.0 ‰). The correction is larger for the experiments using pellets as the water/gas ratio is significantly lower than for the experiments using Pt-rods (96 vs 538, respectively). In terms of 1000 × $\ln^{D}\alpha_{H2O(l)\text{-}H2(g)}$ values these corrections yield changes in the water isotopic composition of ~1 ‰ for catalytic rods and ~6 ‰ for pellets.

3. Results

We present the results as follows. First, we present the precision and accuracy of our measurements and then we present the results of the experiments. We describe our reproducibility and accuracy at length as the values for these set our overall ability to compare and differentiate our results from past studies.

3.1. Results Part 1: Precision and Accuracy of measurement

3.1.1. Precision of δD measurements and 1000 × $\ln^{D}\alpha_{H2O(l)\text{-}H2(g)}$

We estimated the analytical reproducibility (i.e., external precision) of our δD_{H2} measurements by measuring an in-house H_2 standard across all sessions. This exercise yielded a standard deviation (1σ) of 3.2 ‰ (*n* = 102, δD_{H2} = –187.7 ‰; see Appendix Table S3 for details). As such, we estimate that our external precision for δD_{H2} is about ±3 ‰ (1σ).

We estimated the external precision for δD_{H2O} measurements via replicate measurements of the initial waters used in our experiments: milli-Q water (δD_{H2O} = −94.5 ‰, ±1.74 (1σ), *n* = 26) and the enriched water (δD_{H2O} = +349.0 ‰ ±1.13 (1σ), *n* = 4). We also measured the isotopic composition of water following equilibration with H_2 from some Pt-rod experiments (milli-Q water: δD_{H2O} = −95.3 ‰, ±0.90 (1σ), *n* = 23, heavy water: δD_{H2O} = +348.1 ‰ ±1.79 (1σ), *n* = 6). All data used to calculate these numbers are given in Appendix Table S1. Based on these results, we estimate an external precision for δD_{H2O} measurements to typically be between ±0.9 and 1.8 ‰ (1σ).

We are ultimately interested in determining values of 1000 × $\ln^{D}\alpha_{H2O(l)\text{-}H2(g)}$. Uncertainties for this parameter depend both on the uncertainties of δD_{H2} and δD_{H2O} as well as their magnitudes. We estimated the minimum expected uncertainty for experimental measurements of 1000 × $\ln^{D}\alpha_{H2O(l)\text{-}H2(g)}$ with a Monte Carlo error propagation scheme based solely on the external precision of the isotopic measurements detailed above (i.e., excluding additional uncertainties associated with experimental manipulations — this is dealt with separately below). For each experiment, we calculated one million simulations assuming that the milli-Q water has a δD_{H2O} = –94.5 ‰ (unreacted milli-Q water value), and an associated uncertainty of ±0.34 ‰ (1 s.e.). We used the standard error for the water uncertainty as we assume all experiments using a given water source have the same initial value (and thus correlated uncertainty). We assumed the δD_{H2} has an uncertainty of ±3.2 ‰ (1σ). The uncertainty estimated also depends on the value of 1000 × $\ln^{D}\alpha_{H2O(l)\text{-}H2(g)}$, which for our experimental temperature range (3–90 °C) has been estimated previously to range from 1484−1012 ‰ (see Turner et al., 2021). Based on this, we calculated uncertainties of 1000 × $\ln^{D}\alpha_{H2O(l)\text{-}H2(g)}$ values ranging between 9.5–15.5 ‰ (1σ, see Appendix Table S5).

We note that this significant increase for the uncertainty on 1000 × $\ln^D\alpha_{H2O(l)-H2(g)}$ vs. the external precision of ±3.2 ‰ uncertainty (1σ) on the δD_{H2} and 0.34 ‰ (1 s.e.) for the δD_{H2O} of milli-Q water and 0.56 ‰ (1 s.e.) for the δD_{H2O} of the enriched water is due to the large (many hundreds of per mil) difference in the isotopic composition of water versus H_2. As such, the uncertainty on a given experiment using the milli-Q water (which are the majority of experiments; ~90 %) will generally not be better than 9.5 ‰. However, this can be improved upon by replicating experiments at a given temperature.

The uncertainty estimates above are minimum estimates as they are based solely on the reproducibility of our isotopic measurements. We now compare this to an estimate of our experimental reproducibility based on 15 experiments conducted at 10 °C, using both types of catalysts (i.e., Pt rods and Pt-Al pellets), 12 with the milli-Q water (−94.6 ‰) and 3 with heavy water (+349.0 ‰), all of which are bottom brackets. We consider this set of experiments to provide a representative test of our true experimental reproducibility given it involves multiple experiments at the same temperature with variations in many of the experimental variables involved (i.e., different catalyst types and water compositions). We first compare reproducibility of δD_{H2} measured at the end of experiments for those conducted with the same initial $\delta D_{H2O.}$ The δD_{H2} reproducibility of the 12 experiments made with milli-Q water is ±1.9 ‰ (1σ) while for the 3 experiments with heavy water it is ±1.4 ‰ (1σ). As such, reproducibility of δD_{H2} is similar to that of our internal H_2 standard (±3.2 ‰) indicating that the experiments do not increase uncertainty markedly compared to replicate measurements of pure H_2. Once converted to values of 1000 × $\ln^D\alpha_{H2O(l)-H2(g)}$, the uncertainty for all bottom-bracket (i.e., $n = 15$) experiments at 10 °C (regardless of initial water compositions) is ±8.04 ‰ (1σ). We consider this number to be a conservative estimate of the standard deviation for experimental reproducibility (though recall this can be decreased via replication of experiments). This number is similar to that expected based on the Monte Carlo calculations (between about 9.5–15.5 ‰, ±1σ) and, as such, we conclude that our experiments do not, on average, introduce additional uncertainty beyond that based solely and measurement reproducibility.

3.1.2. *Accuracy of δD_{H2} measurements*

Here we present our analysis of the accuracy of our δD_{H2} determinations. We examine this in detail as there are no internationally accepted isotopic reference standards available for molecular hydrogen that are themselves distributed as molecular hydrogen. Rather, δD_{H2} determinations are typically standardized using water standards converted to H_2. It has previously been observed that a lack of internationally available and agreed upon H_2 isotopic standards can create significant (order 10 s of per mil) uncertainties in the accuracy of reported values of molecular hydrogen (Brand and Coplen, 2001). For all measurements sessions, we standardized vs. three H_2 standards with declared δD_{H2} values purchased from Oztech ($\delta D_{H2(VSMOW)}$ = –762.6, −364.1 and −124.8 ‰). Use of these standards ensures internal reproducibility and linearity across the different measurement sessions (Brand and Coplen, 2001).

However, our measurements are only as accurate as the values given for the standards. This is an issue for two reasons: First, when using typical laboratory water compositions (usually 0 ‰ or less in δD), hydrogen in equilibrium with these waters at room temperature will be hundreds of per mil lower in δD vs. the lowest water available with known δD (SLAP with a δD_{H2} = –428 ‰). Second, even if samples of H_2 are normalized against H_2 gases generated from waters with defined values (as was done for the standards used here), measured δD_{H2} of the same gas with an isotopic composition of ~700 ‰ can vary by up to ~50 ‰ between laboratories with a standard deviation between laboratories of ~13 ‰ (Brand and Coplen, 2001). As such, standardization to H_2 gases isotopically calibrated using water standards with defined compositions is not itself sufficient for accurate isotopic determinations of pure H_2. The reasons for this are potentially due to non-quantitative generation of H_2 such that gases are fractionated vs. the source waters — this is discussed in Brand and Coplen (2001) and we refer readers to that study for an overview of these standardization issues. Regardless, there is real potential for inaccuracy in our measured δD_{H2} and something that must be evaluated. Below we present two approaches we took to evaluate this issue.

First, we purchased a second set of H_2 standards from the company ATG (which has now replaced Oztech in providing these standards) with declared δD_{H2} values close to those from Oztech ($\delta D_{H2\ (VSMOW)}$ = –758.7, −362.8 and −123.6 ‰). Both the Oztech and ATG standards were standardized and placed on the VSMOW-SLAP scale via measurement of water standards with known isotopic compositions that were converted to H_2 via reduction over hot uranium. We analyzed these standards at LBNL following our standard practices as well as at Caltech using a high-resolution isotope ratio (Thermo Ultra) mass spectrometer that removes the contribution of the H_3^+ adduct from the mass 3 measurement, which should improve accuracy of measured values across large ranges in δD. Measurements at Caltech are standardized as described in Mangenot et al. (2023). Importantly, based on the study of Mangenot et al. (2023), measurements of water standards converted to H_2 over hot uranium measured on the high-resolution mass spectrometer at Caltech deviate by 0.46 ‰ vs. declared values as a linear difference in δD_{H2} values and 0.02 ‰ in terms of differences in terms of relative D/H ratios over a range of ~1200 ‰ in δD (−428 to +800 ‰). As such, we consider the measurements at Caltech to likely be accurate to <0.5 ‰.

Results of this test between LBNL and Caltech are given in Table 3. The difference between our measurements made at LBNL and Caltech vs. the declared ATG value (measured minus ATG) are as follows: +6.2 and +2.18 ‰ for δD_{H2} = –758.7 ‰; −2.1 and +1.02 ‰ for δD_{H2} = –362.8 ‰; and −4.3 and −0.11 ‰ for δD_{H2} = –123.6 ‰. The average difference between the different laboratories is 1.1 ‰, which we take to indicate good agreement and, thus accuracy, of measurement techniques given the different methods and standardization procedures.

However, one concern is that the deviations between the laboratories are not random but instead a function of the δD of the gases, with the LBNL measurements lower for δD_{H2} = –362.8 and −123.6 ‰ and higher for δD_{H2} = –758.7 ‰ (i.e., the LBNL measurements are not linear with a slope = 1). This makes a testable prediction. Specifically, it predicts that H_2 equilibrated at the same temperature with water ranging by multiple hundred per mil will exhibit differences in 1000 × $\ln^D\alpha_{H2O(l)-H2(g)}$ with a positive relationship between δD_{H2O} and 1000 × $\ln^D\alpha_{H2O(l)-H2(g)}$.

We did this exact test and equilibrated H_2 at the same temperature (specifically 3, 10, 22, 25, 30 and 60 °C) in waters spanning a range of 444 ‰ (−94.6 vs 349.0 ‰; Fig. 3). Given this water δD range our measured 1000 × $\ln^D\alpha_{H2O(l)-H2(g)}$ from 3 to 60 °C, we would predict the differences between measured vs. declared ATG (with measured values at LBNL) would induce differences of between 11 to 16 ‰ in 1000 × $\ln^D\alpha_{H2O(l)-H2(g)}$ with water with higher δD_{H2O} higher in 1000 × $\ln^D\alpha_{H2O(l)-H2(g)}$. We observe, on average, the opposite. We observe that the final averaged 1000 × $\ln^D\alpha_{H2O(l)-H2(g)}$ values of the heavy water minus lighter water differ between −17.4 to +4.82 ‰, with half having positive slopes and half negative slopes vs. δD_{H2O}. The average difference (heavy water minus light water experiments) is −3.94 ±3.58 (1 s.e.) and thus within 2 s.e. uncertainty of zero difference. Based on this, we assume that our measurements are effectively linear with a slope = 1 vs. the correct value. This however does not preclude small (few per mil) constant offsets between labs, which is discussed below. Additionally, based on this test, we consider that the final 1000 × $\ln^D\alpha_{H2O(l)-H2(g)}$ values are independent of the δD_{H2O} of the water used. As such, we averaged 1000 × $\ln^D\alpha_{H2O(l)-H2(g)}$ of a given experiment regardless of the δD_{H2O} value used.

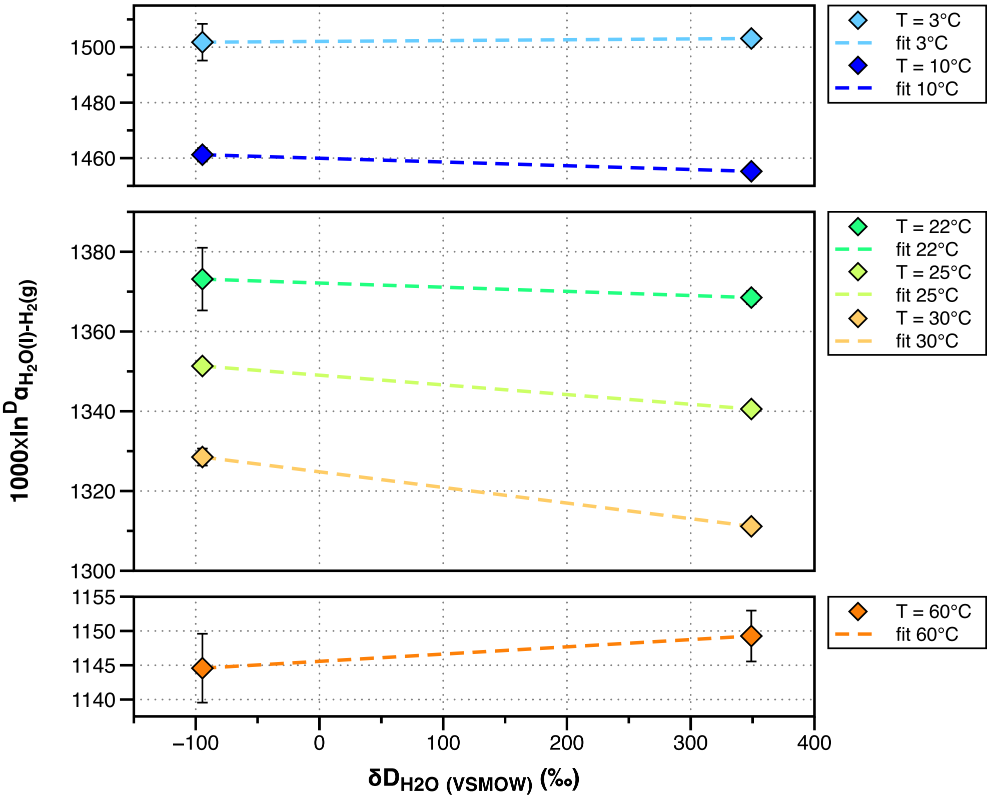

Fig. 3. Average 1000 × $\ln^{D}\alpha_{H2O(l)\text{-}H2(g)}$ values for top and bottom bracket experiments versus the δD of the water (‰). Error bars are ±1 s.e.. If an error bar is not visible, it is smaller than the size of the point.

3.2. Results Part 2: Data from experimental equilibrations

3.2.1. Bracketed experimental results

Final top and bottom bracket values are presented in Fig. 4 and Table 1. If multiple top or bottom experiments were conducted at a given temperature, the value given represents the average of these experiments. Data for individual experiments are given in Appendix Table S2. We now evaluate the success of these experiments in terms of yielding values for hydrogen isotopic equilibrium between H_2 and liquid water.

As noted above, a successfully bracketed experiment is obtained when (*i*) the initial $^{D}\alpha_{H2O(l)\text{-}H2(g)}$ is smaller (bottom bracket) or higher (top bracket) than the final $^{D}\alpha_{H2O(l)\text{-}H2(g)}$ value and (*ii*) top and bottom bracketing experiments yield the same value for $^{D}\alpha_{H2O(l)\text{-}H2(g)}$ value within a defined uncertainty (O'Neil, 1986). Condition (*i*) was satisfied for all experiments as starting bottom values of $^{D}\alpha_{H2O(l)\text{-}H2(g)}$ were always between 1.184 and 1.763 (depending of the water used, see section 2.2) and less than the lowest measured $^{D}\alpha_{H2O(l)\text{-}H2(g)}$ (~2.7 at 90 °C). Additionally, we verified that top brackets always started above the final desired temperature (see Appendix Table S2).

We evaluate the second condition by examining if any experiments yielded differences between the top and bottom brackets that deviate more than expected given our typical reproducibility for experiments. Such could indicate a failure of the two brackets to both reach equilibrium. We use a typical experimental reproducibility of ±8.04 ‰ (1σ) estimated from bottom experiments at 10 °C (see section 3.1.1). We consider that any pairs of averaged final top and bottom bracket 1000 × $\ln^{D}\alpha_{H2O(l)\text{-}H2(g)}$ values that yield two standard deviations less than 16.1 ‰ (i.e., ±2σ where 1σ = 8.04 ‰) were successfully bracketed. Using this cutoff, all experiments can be considered successfully bracketed with experiments at 10, 15, 20, 25, 30, 35, 40, 60 and 70 °C all yielding standard deviations <1σ (8.04 ‰) and the experiments at 3, 50, and 90 °C yielding standard deviations <2σ (16.1 ‰) (Table 2). We note that the results at 3 °C are bottom experiments only (*n* = 5), including 4 with milli-Q water and one with heavy water. This is because this is the lowest temperature we used to create top brackets from other experimental temperatures. We use this value in our calibration despite it not being bracketed as it yields results consistent with the temperature dependence determined from other bracketed experiments and was constrained in multiple different experiments. Its inclusion does not influence the values of our calibration for 1000 × $\ln^{D}\alpha_{H2O(l)\text{-}H2(g)}$ values vs. 1/T (presented below) beyond 1 s.e..

3.2.2. Calculation of 1000 × $\ln^{D}\alpha_{H2(g)\text{-}H2O(l)}$ values at equilibrium as a function of temperature

We present our estimates for equilibrium 1000 × $\ln^{D}\alpha_{H2O(l)\text{-}H2(g)}$ values and associated experimental temperatures in Table 2 and Fig. 5A. These were calculated by taking the average value of already averaged top and bottom bracket experiments at a given temperature.

We created a calibration of 1000 × $\ln^{D}\alpha_{H2O(l)\text{-}H2(g)}$ vs. temperature by regressing the values of 1000 × $\ln^{D}\alpha_{H2O(l)\text{-}H2(g)}$ values vs. 1/T (in Kelvin) for 3–90 °C temperature range. We do this as a weighted least squares (WLS) regression as the standard error varies between experiments. This yields the following equation ($R^2 = 0.999$):

$$1000\times\ln^{D}\alpha_{H2O(l)-H2(g)} = -526.48 + \frac{559,316}{T} \tag{3}$$

The residuals of our final averaged 1000 × $\ln^{D}\alpha_{H2O(l)\text{-}H2(g)}$ values and our WLS fit range from −18.1 to +15.0 ‰ with an average of 1.2 ±7.9 ‰ (1σ). We observe no pattern of the residuals vs. 1/T (Fig. 5B) indicating that over this temperature range, a linear fit of 1000 × $\ln^{D}\alpha_{H2O(l)\text{-}H2(g)}$ vs. 1/T is appropriate. The uncertainties on the slope and intercept are ±8,97097 and ±30.52 (1s.e.) respectively.

4. Discussion

We now compare our calibration to prior experimental and

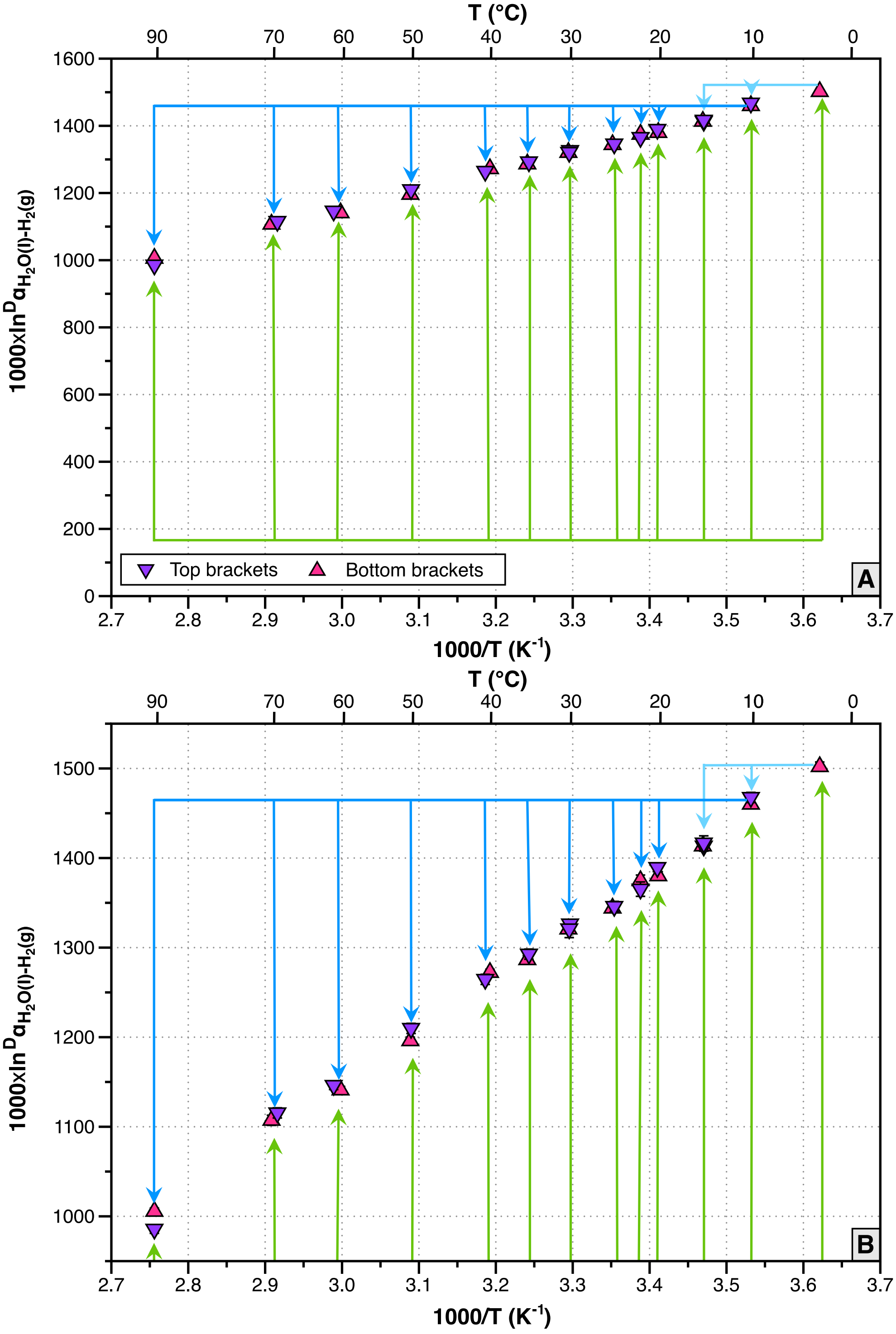

Fig. 4. A) Final values of 1000 × $\ln^D\alpha_{H2O(l)\text{-}H2(g)}$ for top-bracket (downward purple triangles) and for final bottom-bracket (upward pink triangles) experiments versus 1000/T (K^{-1}). B) Same as A) but zoomed in. Light blue lines indicate pre-equilibrations conducted at 3 °C while dark blue lines indicate pre-equilibrations at 10 °C. Green lines represent the initial gas composition value for bottom experiments. Error bars correspond to ±1 s.e. when experiments included multiple top or bottom experiments. If only one top or bottom experiment was conducted, error bars are ±1σ as calculated via the Monte Carlo error propagation scheme described in the main text. If an error bar is not visible, it is smaller than the size of the point.

theoretical calculations of equilibrium values of 1000 × $\ln^D\alpha_{H2O(l)\text{-}H2(g)}$. These comparisons are given in Fig. 6 (experimental) and Fig. 7 (theoretical). Following these comparisons, we provide a recommended set of equations for the temperature dependence of 1000 × $\ln^D\alpha_{H2O(l)\text{-}H2(g)}$ for use in future geochemical studies.

4.1. Comparison to previous experimental studies and the implications for our understanding of the accuracy of experimental determinations of $\ln^D\alpha_{H2O(l)\text{-}H2(g)}$

We first compare our experimental data and calibration to prior experimental work of Suess (1949), Cerrai et al. (1954), and Rolston

Table 1
Initial and final averaged $^{D}\alpha_{H2O(l)\text{-}H2(g)}$ and 1000 × $\ln^{D}\alpha_{H2O(l)\text{-}H2(g)}$ values of top bracket experiments and of bottom bracket experiments.

Bracket type	*n* measure	*n* experiment	Starting T (°C)	Final T (°C)	Equilibration time (days)	Final. 1000 × $\ln^{D}\alpha_{H2O(l)\text{-}H2(g)}$	±1σ	±1s.e.	$^{D}\alpha_{H2O(l)\text{-}H2(g)}$
Bottom*	11	5	n/a	3.0	11–24	1502.05	11.54	5.16	4.491
Top	4	2	3.0	10.0	15	1467.63	4.61	5.69	4.339
Bottom*	21	15	n/a	10.0	14–28	1460.11	8.04	2.08	4.307
Top	2	2	10.0	15.0	14	1413.35	3.65	5.69	4.110
Top	1	1	3.0	15.0	14	1416.73	8.04	8.04	4.124
Bottom	4	1	n/a	15.1	8	1413.45	3.78	4.02	4.110
Top	3	1	10.0	20.1	8	1389.42	3.24	4.64	4.013
Bottom	3	1	n/a	20.0	8	1380.16	2.08	4.64	3.976
Top	1	1	10.0	22.0	4	1365.28	8.04	8.04	3.917
Bottom*	6	2	n/a	22.0	5	1374.76	8.83	6.24	3.954
Top*	8	2	10.0	25.0	8	1345.95	7.62	5.69	3.842
Bottom	3	1	n/a	25.2	8	1344.09	8.02	4.63	3.835
Top	4	1	10.0	30.2	4	1326.39	2.97	4.64	3.767
Top*	6	2	22.0	30.3	4	1320.90	13.8	9.76	3.747
Bottom	3	1	n/a	30.4	4	1320.75	4.65	4.64	3.746
Top	3	1	10.0	35.2	4	1292.72	7.13	5.69	3.643
Bottom	3	1	n/a	35.4	4	1286.49	7.88	4.64	3.620
Top	2	1	10.0	40.7	4	1264.54	2.63	5.69	3.542
Bottom	19	5	n/a	40.1	5	1272.27	4.51	3.60	3.569
Top	6	2	10.0	50.5	3	1209.80	5.69	5.69	3.353
Bottom	4	1	n/a	50.6	3–5	1196.01	2.98	4.02	3.307
Top*	8	3	10.0	61.4	5	1146.14	7.60	4.64	3.141
Bottom	4	1	n/a	60.4	4	1141.06	5.40	4.02	3.130
Top	6	2	10.0	69.8	2	1115.47	1.38	5.69	3.051
Bottom	7	2	n/a	70.7	4	1107.21	2.23	5.69	3.026
Top	3	1	10.0	89.7	2	985.61	2.17	4.64	2.679
Bottom	5	1	n/a	89.7	52 h	1005.58	5.57	3.60	2.733

n/a: no starting temperature, initial value corresponds to the starting gas composition
*average values including heavy water experiments (δD_{H2O} = +349.0 ‰).
[a]: If the measured standard deviation measured is less than our typical uncertainty (8.04‰), then we use the typical uncertainty to calculate the standard error. For experiments where n ≥ 1, we used n experiments to calculate the standard error, for n experiment = 1, we used n measures.

Table 2
Final averaged 1000 × $\ln^{D}\alpha_{H2O(l)\text{-}H2(g)}$ values of experiments. More significant digits are provide in the Mendeley Data bank at https://doi.org/10.17632/63bmz2z8v9.1 and such are needed to match our provided fits.

T (°C)	$^{D}\alpha_{H2O(l)\text{-}H2(g)}$	±1σ	±1s.e.	1000 × $\ln^{D}\alpha_{H2O(l)\text{-}H2(g)}$	±1σ	±1s.e.
3*	4.491	0.052	0.052	1502.05	11.54	5.16
10.0	4.323	0.023	0.016	1463.87	5.32	3.76
15.0	4.113	0.005	0.003	1414.25	1.12	0.56
20.1	3.994	0.026	0.018	1384.79	6.55	4.63
22.0	3.936	0.027	0.019	1370.02	6.71	4.74
25.1	3.838	0.005	0.004	1345.02	1.32	0.93
30.3	3.752	0.008	0.005	1322.20	2.04	1.44
35.3	3.631	0.016	0.011	1289.61	4.41	3.12
40.4	3.555	0.019	0.014	1268.41	5.46	3.86
50.6	3.330	0.033	0.023	1202.91	9.75	6.90
60.9	3.138	0.011	0.008	1143.60	3.59	2.54
70.3	3.038	0.018	0.013	1111.34	5.84	4.13
89.7	2.706	0.038	0.027	995.59	14.12	9.98

*only bottom-bracket experiments.

Table 3
Averaged isotopic composition of $H_{2(g)}$ from ATG standards measured at the LBNL and Caltech.

δD_{H2} labelled value	δD_{H2} meas. LBNL	±1σ	δD_{H2} meas. Caltech	±1s.e.
−123.6	−127.9	1.96	−123.71	0.25
−362.8	−364.9	2.45	−361.78	0.26
−758.7	−752.5	1.18	−756.52	0.12

et al. (1976). We do this comparison by always taking the difference between the 1000 × $\ln^{D}\alpha_{H2O(l)\text{-}H2(g)}$ experimental values of these studies minus our WLS fit. As mentioned above, only Rolston et al. (1976) experimentally measured 1000 × $\ln^{D}\alpha_{H2O(l)\text{-}H2(g)}$ values directly. The experiments of Suess (1949) and Cerrai et al. (1954) were done in the gas phase (i.e., 1000 × $\ln^{D}\alpha_{H2O(g)\text{-}H2(g)}$). We have converted these values to 1000 × $\ln^{D}\alpha_{H2O(l)\text{-}H2(g)}$ using the experimental calibration of $^{D}\alpha_{H2O(l)\text{-}H2O(g)}$ from Horita and Wesolowski (1994).

Only one experimental value from Suess (1949) is comparable (at 80 °C) as they provide experimental data mainly for T>100 °C. This point agrees within 6.9 ‰ of our calibration (WLS fit). The experimental data of Cerrai et al. (1954) for the 51–97 °C temperature range differ from our WLS fit from −68.2 to −6.9 ‰, with an average difference of −30.5 ±23.9 ‰ (1σ). Much of this disagreement stems from two experiments from their work at 59 and 64 °C (Fig. 6). These experiments have been assumed to be erroneous by later studies and excluded from any comparisons (e.g., Rolston et al., 1976; Bardo and Wolfsberg, 1976; Turner et al., 2021) — though we note there is not a specific reason for excluding these beyond them differing by tens of per mil from other nearby (in terms of temperature) points in Cerrai et al. (1954). Regardless, if these two points are excluded from the comparison, the average difference of the Cerrai et al. (1954) data vs. our WLS fit is −18.4 ±10.1 ‰ (1σ).

The experimental data of Suess (1949) and Cerrai et al. (1954), when used in geochemical studies, are not used directly. Rather, polynomial

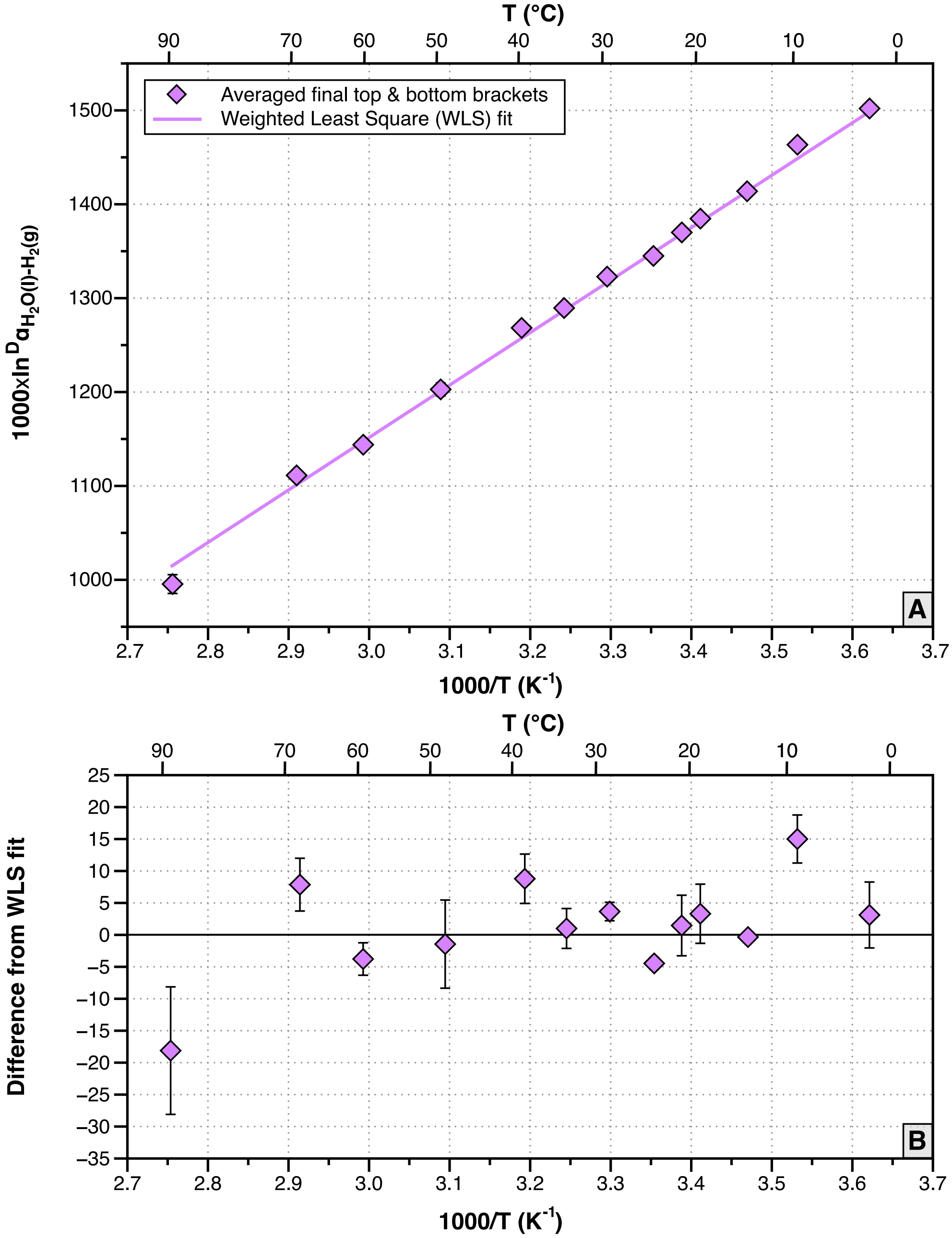

Fig. 5. A) Average of final top and bottom 1000 × ln$^D\alpha_{H2O(l)\text{-}H2(g)}$ experimental values versus 1000/T (K^{-1}) and the associated weighted last squares (WLS) linear fit (1000 × ln$^D\alpha_{H2O(l)\text{-}H2(g)}$ = –526.48 + 559,316/T). Error bars are ±1 s.e. or are smaller than the point size if not shown. B) Difference in per mil (‰) between final averaged top and bottom 1000 × ln$^D\alpha_{H2O(l)\text{-}H2(g)}$ values and the weighted last squares linear fit versus 1000/T (K^{-1}) with error bars ±1 s.e. If not shown, they are smaller than the size of the point.

regressions of the dependence of $^D\alpha_{H2O(l)\text{-}H2(g)}$ on temperature are used. It is our understanding that most recent studies have used the regressions provided in Horibe and Craig (1995). These regressions are given as a linear dependence of $^D\alpha_{H2O(g)\text{-}H2(g)}$ on 1/T (as opposed to the logarithm of $^D\alpha_{H2O(g)\text{-}H2(g)}$) and, in some cases, extrapolate them outside of the calibrated range to lower temperatures (Fig. 6). Although such an extrapolation can be problematic, we provide and compare to these lines from 90–3 °C for completeness as such extrapolations are used in various geochemical studies. To do this, we apply the calibration of $^D\alpha_{H2O(l)\text{-}H2O(g)}$ from Horita and Wesolowski (1994) to convert calibrations to $^D\alpha_{H2O(l)\text{-}H2(g)}$. From 3–90 °C, at 1 °C increments, the fit to the Suess (1949) data by Horibe and Craig (1994) differs from the WLS by on average −11.4 ±9.9 (1σ) (range of −29.9 to +3.9 ‰) while those of Cerrai et al. (1954) (excluding the two potentially erroneous points indicated above) differ from the WLS by on average −31.5 ±14.6 ‰ (1σ) (range of −58.1 to −8.2 ‰).

We next compare our results to those from Rolston et al. (1976), which we consider most similar both in temperature range and approach of equilibrating molecular hydrogen with liquid water. We observe that the experimental data of Rolston et al. (1976) (temperature range of 6–95 °C) differ from our WLS fit from −36.5 to +27.3 with an average of −6.1 ±13.7 ‰ (1σ). Similar to some of the data from Cerrai et al. (1954), a few experiments (18, 24 and 30 °C) from Rolston et al. (1976) differ more than 20 ‰ compared to our WLS fit (Fig. 6B). Five of our experiments (15, 22, 30, 40 and 61 °C) were conducted at the same temperatures (i.e., within 1 °C) as Rolston et al. (1976). For these specific temperatures, we observe that experimental data from Rolston et al. (1976) are typically lower than our experimental 1000 × ln$^D\alpha_{H2O(l)\text{-}H2(g)}$

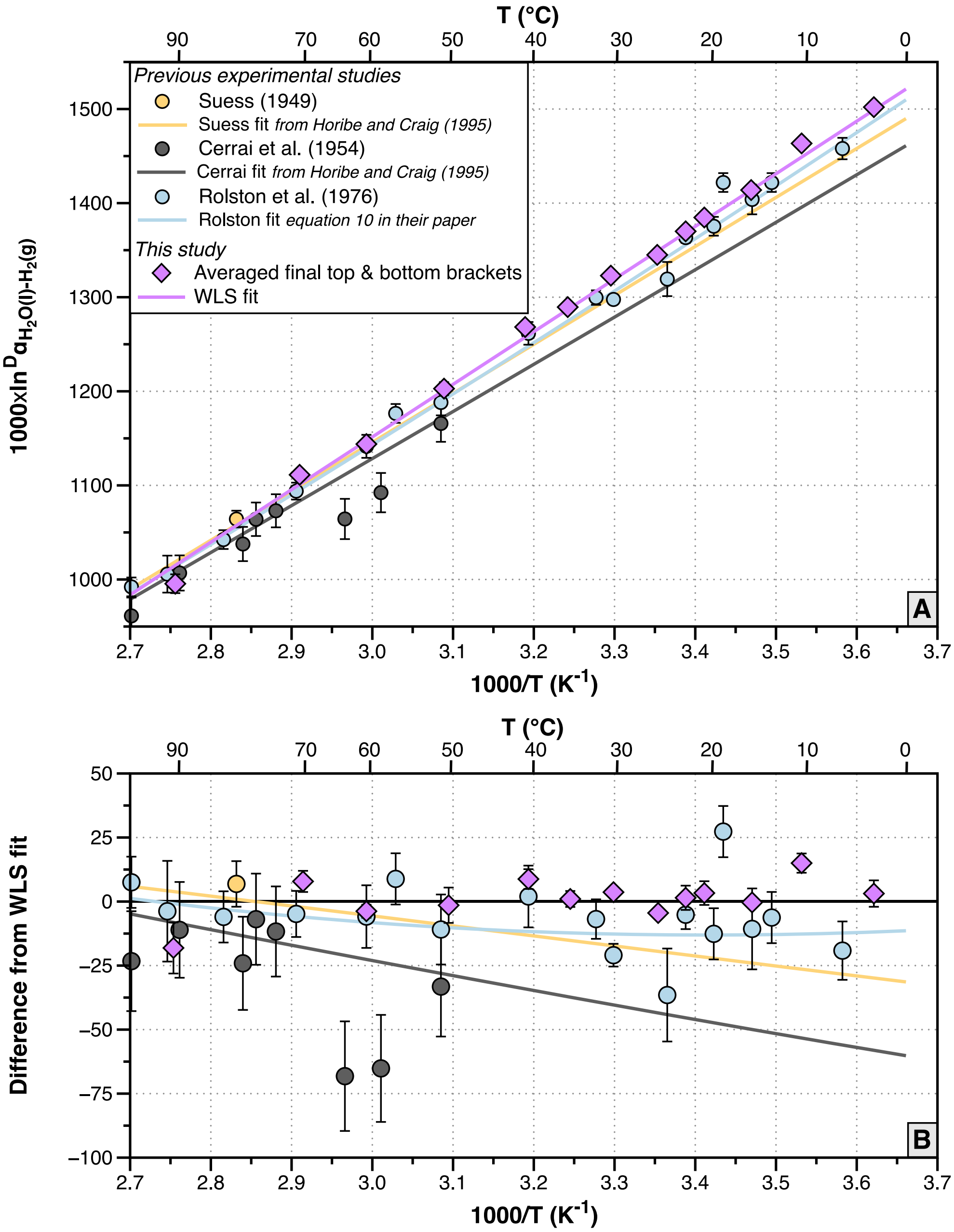

Fig. 6. A) Comparison of the averaged top and bottom bracket $1000 \times \ln^{D}\alpha_{H2O(l)-H2(g)}$ values from this study (purple diamonds) and our WLS fit (purple line) vs. data from previous experimental studies. Error bars for our data are ±1 s.e. and error bars for data from Suess (1949), Cerrai et al. (1954) and Rolston et al. (1976) are ±1σ as reported in the original studies. B) Difference in per mil (‰) relative to the WLS fit (extrapolated at T < 3°C and T > 90 °C). Fits for experimental data from Suess (1949) and Cerrai et al. (1954) are taken from Horibe and Craig, (1995) as given in Fig. 6 from their paper. The fit from experimental data for Rolston et al. (1976) is from equation (10) given in that study. Note the data from Suess (1949) and Cerrai et al. (1954) were given in the original studies as $^{D}\alpha_{H2O(v)-H2(g)}$. We converted them to $^{D}\alpha_{H2O(l)-H2(g)}$ using the calibration for $^{D}\alpha_{H2O(l)-H2O(g)}$ from Horita and Wesolowski (1994). If an error bar is not visible, it is smaller than the size of the point.

values, with differences ranging from −24.6 to −2.10 ‰ and with an average difference of −10.1 ±8.6 ‰ (1σ).

A key question is whether the experiments presented here differ significantly from prior experimental results and thus justify a separate calibration vs. combining some or all of the previous studies with the results presented to form a unified calibration. We only address this here for temperatures from 3-90 °C, i.e., within our calibrated range. Given that data from Suess (1949) only overlap at one temperature (80 °C), we do not conduct this comparison for this study.

We determine if the calibrations are significantly different between our experiments and that of Cerrai et al. (1954) and Rolston et al. (1976) by examining whether the slopes and intercepts of the calibrations solely for overlapping temperatures (i.e., 3–90 °C) are within 2 s.e. uncertainty. This is done using an interaction term and multivariate linear regression (see Appendix A.2 of the Supplementary Material). We find that the slopes and intercepts derived for our data differ beyond 2 s.e. vs. those from Cerrai et al. (1954) and Rolston et al. (1976). We note that in doing this, we are not doing a weighted regression as we do not have good estimates of uncertainty for individual experiments from these prior experiments. Regardless, based on this analysis, we consider our experiments to be sufficiently different from prior work to justify a separate calibration that does not include the prior data.

Despite considering the data to be different, it is important to note that these differences are relatively small, typically <20 ‰ (−18.4 ‰ on

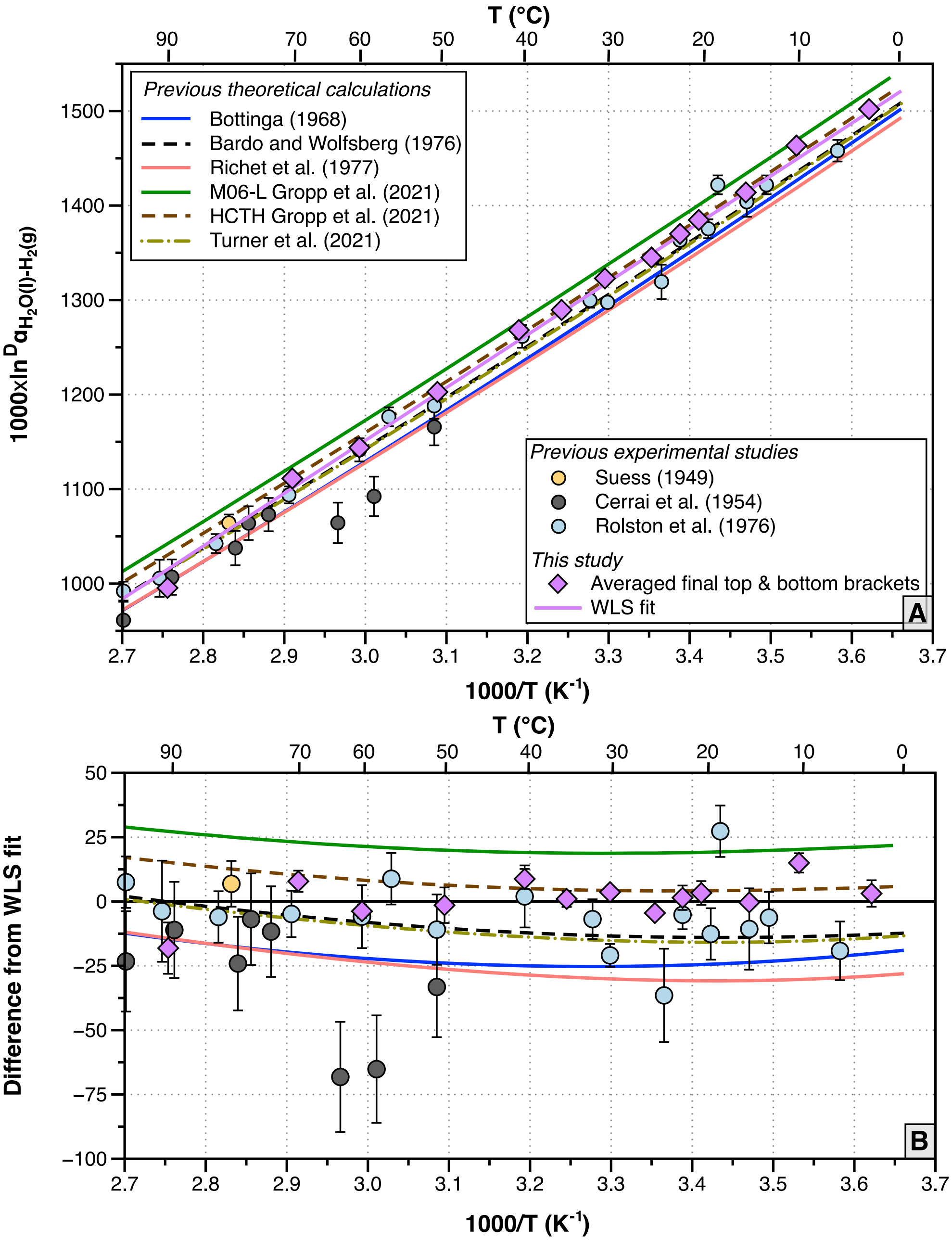

Fig. 7. A) Comparison of the averaged top and bottom bracket $1000 \times \ln {}^{D}\alpha_{H2O(l)\text{-}H2(g)}$ values from this study (purple diamonds) and our WLS fit (purple line) vs. values from previous theoretical studies. Error bars for our data are ±1 s.e. and error bars for data from Suess (1949), Cerrai et al. (1954) and Rolston et al. (1976) are ±1σ as reported in the original studies. B) Difference in per mil (‰) relative to the WLS fit for the experimental data (points) and theoretical calculations (curves). Note the data from Suess (1949) and Cerrai et al. (1954) and all theoretical studies were originally given as ${}^{D}\alpha_{H2O(v)\text{-}H2(g)}$. We converted them to ${}^{D}\alpha_{H2O(l)\text{-}H2(g)}$ using the calibration for ${}^{D}\alpha_{H2O(l)\text{-}H2O(g)}$ from Horita and Wesolowski (1994). If an error bar is not visible, it is smaller than the size of the point.

average for Cerrai et al., 1954, excluding points at 59 and 64 °C, and −6.1 ‰ on average for Rolston et al., 1976). We consider this agreement quite remarkable given the long time span these experiments cover (~75 years), different techniques used for equilibrations, and different techniques for measurements. As such, another way to describe the data is to state that within about 20 ‰ from 0–100 °C, the values of $1000 \times \ln^{D}\alpha_{H2O(l)\text{-}H2(g)}$ are well constrained experimentally. It is only once smaller (<20 ‰) differences are examined that deviations appear.

4.2. Comparison to previous theoretical calculations and the associated implications for future theoretical studies

We now turn to a comparison of our experimental data vs. previous theoretical calculations (Fig. 7). A question is whether the experiments described here agree with the theoretical calculations presented in the past few years and if various corrections such as the Diagonal Born-Oppenheimer correction (DBOC) are necessary to achieve agreement between theory and experiment. Critical to this comparison is an understanding of the accuracy of our measurements — i.e., how different must a theoretical calculation be vs. our experiments to be considered distinct? We consider this first before discussing the theoretical treatments.

Based on our analysis of the ATG standards, we consider it typical that δD_{H2} measurements between laboratories will differ up to ~±4‰ (based on the differences in individual standard values measured at the LBNL and Caltech (Table 3). For the range of ${}^{D}\alpha_{H2O(l)\text{-}H2(g)}$ measured here from 3–90 °C (∼4.5 to 2.7) and using a water δD of ∼−100 ‰, a difference of 4 ‰ in δD_{H2} translates to differences in $1000 \times \ln^{D}\alpha_{H2O(l)\text{-}H2(g)}$ of 12–20 ‰. As such, we consider differences between experimental results and theory to within ∼10 to 20 ‰ to not be distinguishable given current abilities to standardize and accurately measure δD_{H2} to within a ∼5 per mil.

With this in mind, we now compare our $1000 \times \ln^{D}\alpha_{H2O(l)\text{-}H2(g)}$ calibration (WLS fit from 3 to 90 °C) to various published theoretical calculations (Fig. 7). We do this comparison by computing the value of $1000 \times \ln^{D}\alpha_{H2O(l)\text{-}H2(g)}$ at 1 °C increments for both our calibration and the given theoretical calibration (generally based on a polynomial fit given in the study or that we calculated) and then taking the difference ($1000 \times \ln^{D}\alpha_{H2O(l)\text{-}H2(g)}$ theoretical values minus WLS fit) over that range. In doing this, as above, we convert theoretical calculations of $1000 \times \ln^{D}\alpha_{H2O(g)\text{-}H2(g)}$ to $1000 \times \ln^{D}\alpha_{H2O(l)\text{-}H2(g)}$ using the experimental calibration of $1000 \times \ln^{D}\alpha_{H2O(l)\text{-}H2O(g)}$ from Horita and Wesolowski (1994). We observe the following average (and 1σ) differences: −22.1 ±3.1 ‰ (min: −25.3, max: −14.5 ‰) for Bottinga (1968), −9.6 ±4.4 ‰ (min: −14.0, max: −0.1 ‰) for Bardo and Wolfsberg (1976), −25.4 ±5.2 ‰ (min: −30.8, max: −14.3 ‰) for Richet et al. (1977), +21.2 ±2.4 ‰ (min: +18.7, max: +27.0 ‰) and +7.4 ±3.4 ‰ (min: +4.1, max: +14.9 ‰) for M06-L and HCTH fits from Gropp et al. (2021) and −11.0 ±4.6 ‰ (min: −15.9, max: −1.3 ‰) for Turner et al. (2021).

To summarize these results, the theoretical studies generally agree within ±20 to 25 ‰ of the experimental results, and most are within or close to the 12–20 ‰ accuracy range of our experimental calibration based on δD_{H2} accuracy. The three studies that agree most closely (i.e., within ±11 ‰) are those from Gropp et al., (2021) based on the HCTH model and those Bardo and Wolfsberg (1976) and Turner et al. (2021) which incorporated both corrections for anharmonicity and the Diagonal Born-Oppenheimer Correction. In the study of Gropp et al. (2021), the HCTH model was used only for evaluation purposes of another DFT-based model and we consider the agreement here likely fortuitous. There is also good agreement between the experimental work presented vs. those from Bardo and Wolfsberg (1976) and Turner et al. (2021) with average differences of −9.6 and −11.0 ‰ respectively vs. our experimental calibration. These are the only studies to include both corrections for anharmonicity and the Diagonal Born-Oppenheimer Correction. We take this to indicate that such corrections are critical for getting theory and experiment to consistently agree at the ∼10 ‰ level for studies involving isotopic fractionations of hydrogen.

4.3. *Recommended calibrations for $^{D}\alpha_{H2O(l)\text{-}H2(g)}$ from 0 to 374 °C and associated implications in environmental systems*

The final point we take up is what calibration should be used to calculate $^{D}\alpha_{H2O(l)\text{-}H2(g)}$ in future geochemical studies. From 3–90 °C, we propose that the fit provided in equation (3) based on our experiments only is appropriate to use and preferrable to prior experimental results as it is based on experiments and measurements that involve modern isotopic techniques and standardization practices. For temperatures from 0–3 °C and above 90 °C and up to the critical point of water, we recommend using calibration of Turner et al. (2021) based on PIMC calculations with the DBO correction and adding an offset term to incorporate constraints based on our experimental data. This approach follows that of Clayton and Kieffer (1991) and allows us to use our experimental calibration to offset the theoretically expected curvature of $1000 \times \ln^{D}\alpha_{H2O(l)\text{-}H2(g)}$ vs. 1/T to higher temperatures. We do this following the approach outlined in Turner et al. (2021) in which we do not modify the terms in the polynomial that modify a temperature dependence and instead only offset the constant additive term. This results in a constant additive offset of 15.79 ‰ vs. theory alone such that the equation is:

$$1000 \times \ln^{D}\alpha_{H2O(l)-H2(g)} = \frac{7.9443 \times 10^{12}}{T^4} - \frac{8.7772 \times 10^{10}}{T^3} + \frac{3.8504 \times 10^{8}}{T^2} - \frac{2.6650 \times 10^{5}}{T} + 217.87 \tag{4}$$

The residuals of the $1000 \times \ln^{D}\alpha_{H2O(l)\text{-}H2(g)}$ values given by our WLS fit (equation (3)) and equation (4) for the overlapping temperature range (3–90 °C) vary from −14.0 to +0.56 ‰ with an average of −4.30 ±4.61 ‰ (1σ). This average and range were found by calculating the value of $1000 \times \ln^{D}\alpha_{H2O(l)\text{-}H2(g)}$ at 1 °C increments from 3-90 °C and calculating these statistics on these points.

As discussed in the introduction, significant differences exist between previously published experimental and theoretical calibrations of $1000 \times \ln^{D}\alpha_{H2O(l)\text{-}H2(g)}$. We close here with an examination of how much the calibrations presented here differ from prior calibrations in terms of estimated temperatures or isotopic compositions. I.e., what differences would one find if this calibration is used in a given study vs. using a previously published calibrations and would it influence one's interpretations? At low temperatures (∼0°C), deviations using other calibrations vs. this study (equation (3)) are as large as 10 °C at 0 °C vs. 5 °C at 100 °C. If we apply equation (4), differences increase up to ∼30 °C around the critical point of water. As such, these deviations are sufficient to change interpretations of depths of H_2 equilibration in the subsurface of 200 m to a kilometer for a typical geotherm of ∼25 °C/km. An alternative way to look at this is as follows. If, for example, an independent estimate of equilibration temperature and δD_{H2} was determined (such as via clumped isotopic studies of D_2; e.g., Popa et al., 2019; Mangenot et al., 2023), estimates of the isotopic composition of the water with which it equilibrated would vary by up to 60 ‰ at 0 °C, 40 ‰ at 100 °C, and 35 ‰ at the critical point of water. These are all significantly beyond measurement precision and would influence interpretations of the origin of fluids that equilibrated with the H_2. For example, it would one's interpretation of whether samples of H_2 formed or equilibrated at the sediment–water interface in the ocean vs. hundreds of meters below the seafloor, equilibrated with meteoric or seawater-derived fluids, or equilibrated in a supercritical or subcritical fluid in hydrothermal systems.

5. Summary and conclusion

We presented an experimental calibration of equilibrium values of $^{D}\alpha_{H2O(l)\text{-}H2(g)}$ from 3 to 90 °C. Experiments were accelerated using platinum catalysts and bracketed to verify equilibrium was reached. Unlike past experimental efforts, isotopic measurements were made using standard stable isotopic techniques and measured relative to internationally traceable standards. Results agree within ∼20 ‰ on average of prior experimental results of Suess (1949), Cerrai et al. (1954) and Rolston et al. (1976) but are statistically different. The results typically agree within 25 ‰ of prior theoretical calculations with consistently better agreement observed (<11 ‰) with prior theoretical results that incorporate both anharmonic corrections and the Diagonal Born-Oppenheimer correction, indicating that these may be needed in order for theoretical calculations to achieve the highest-level agreement with experiments for hydrogen isotope equilibrium. We presented two calibrations of $^{D}\alpha_{H2O(l)\text{-}H2(g)}$ vs. temperature based on our experimental results, one for 3–90 °C based solely on the experiments, and one for temperatures from 0–374 °C that incorporates both the theoretically expected dependence of $^{D}\alpha_{H2O(l)\text{-}H2(g)}$ on temperature and our experimental measurements.

We conclude that from 3–90 °C and at the ∼±20–30 ‰ level, experiments and theory that span the past 70 years are in general agreement indicating that at this level (∼3% relative), $^{D}\alpha_{H2O(l)\text{-}H2(g)}$ is well constrained. However, when accuracy at the <∼10 ‰ level is needed, use of both the highest level of theory and/or experiments conducted with modern techniques is likely necessary.

CRediT authorship contribution statement

Flora Hochscheid: Writing – review & editing, Writing – original draft, Visualization, Validation, Methodology, Investigation, Formal analysis, Conceptualization. **Andrew C. Turner:** Writing – review & editing, Validation, Methodology, Formal analysis. **Noam Lotem:** Investigation. **Markus Bill:** Writing – review & editing, Methodology, Investigation. **Daniel A. Stolper:** Writing – review & editing, Validation, Supervision, Methodology, Funding acquisition, Formal analysis, Conceptualization.

Data availability

Data are available through Mendeley Data at https://doi.org/10.17632/63bmz2z8v9.1.

Declaration of competing interest

The authors declare that they have no known competing financial interests or personal relationships that could have appeared to influence the work reported in this paper.

Acknowledgements

This material is based upon work supported by U.S. Department of Energy, Office of Science, Office of Basic Energy Sciences, Chemical Sciences, Geosciences, and Biosciences Division, under Award Numbers DE-AC02-05CH11231 and DE-SC0022949. We thank Nina Golombek (UC Berkeley) for help translating Suess (1949). We also acknowledge and thank John Eiler (Caltech) for valuable discussion and access to the laboratory in the Division of Geological and Planetary Sciences at Caltech for δD_{H_2} measurements on the 253 Ultra. We also thank Matthieu Clog and two anonymous reviewers for their thoughtful comments.

Appendix A. Supplementary material

Supplementary material to this article can be found online. The Appendix contains five supplementary tables (Table S1 – S5); The (python) script for the Monte Carlo simulation described in section 3.1.1; And one pdf file with the following subsections: A.1 demonstrates that sample storage does not modify the isotopic composition of H_2; A.2 provides details on how we determined whether various experimental studies differ at a statistically significant level. Table S1 presents the isotopic composition of $H_2O_{(l)}$ measured before and after $H_2O_{(l)}$-$H_{2(g)}$ experiments. Table S2 presents the individual mass spectrometric measurements of all top and bottom bracket experiments of this study. Table S3 presents both in-house (internal) and certified δD_{H_2} standards measured as part of this study. Table S4 presents both the in-house and certified δD_{H_2O} standards measured in this study. Table S5 contain estimated uncertainties from Monte Carlo simulation for various top and bottom-bracket experiments. Supplementary material to this article can be found online at https://doi.org/10.1016/j.gca.2025.02.029.

References

Aftab, A., Hassanpouryouzband, A., Xie, Q., Machuca, L.L., Sarmadivaleh, M., 2022. Toward a fundamental understanding of geological hydrogen storage. Ind. Eng. Chem. Res. 61 (9), 3233–3253.

Amirthan, T., Perera, M.S.A., 2023. Underground hydrogen storage in Australia: a review on the feasibility of geological sites. Int. J. Hydrogen Energy 48 (11), 4300–4328.

Bardo, R.D., Wolfsberg, M., 1976. A theoretical calculation of the equilibrium constant for the isotopic exchange reaction between water and hydrogen deuteride. J. Phys. Chem. 80 (10), 1068–1071.

Bigeleisen, J., Mayer, M.G., 1947. Calculation of equilibrium constants for isotopic exchange reactions. J. Chem. Phys. 15 (5), 261–267.

Bottinga, Y., 1968. Hydrogen isotope equilibriums in the system hydrogen-water. J. Phys. Chem. 72 (12), 4338–4340.

Bradley, A.S., Summons, R.E., 2010. Multiple origins of methane at the Lost City Hydrothermal Field. Earth Planet. Sci. Lett. 297 (1–2), 34–41.

Brand, W.A., Coplen, T.B., 2001. An interlaboratory study to test instrument performance of hydrogen dual-inlet isotope-ratio mass spectrometers. Fresenius J. Anal. Chem. 370, 358–362.

Cerrai, E., Marchetti, C., Renzoni, R., Roseo, L., Silvestri, M., Villani, S., 1954. A thermal method for concentrating heavy water. Nuclear engineering, Part I. In: Chem. Eng. Progr. Symposium Ser. Laboratori. CISE, Milan, Italy, pp. 271–280.

Charlou, J.L., Donval, J.P., Fouquet, Y., Jean-Baptiste, P., Holm, N., 2002. Geochemistry of high H2 and CH4 vent fluids issuing from ultramafic rocks at the Rainbow hydrothermal field (36 14′ N, MAR). Chem. Geol. 191 (4), 345–359.

Clayton, R.N., Kieffer, S.W., 1991. Oxygen isotopic thermometer calibrations. In Stable isotope geochemistry: A tribute to Samuel. Epstein 3, 3–10.

Etiope, G., Samardžić, N., Grassa, F., Hrvatović, H., Miošić, N., Skopljak, F., 2017. Methane and hydrogen in hyperalkaline groundwaters of the serpentinized Dinaride ophiolite belt, Bosnia and Herzegovina. Appl. Geochem. 84, 286–296.

Foustoukos, D.I., Mysen, B.O., 2012. D/H fractionation in the H2–H2O system at supercritical water conditions: Compositional and hydrogen bonding effects. Geochim. Cosmochim. Acta 86, 88–102.

Gropp, J., Iron, M.A., Halevy, I., 2021. Theoretical estimates of equilibrium carbon and hydrogen isotope effects in microbial methane production and anaerobic oxidation of methane. Geochim. Cosmochim. Acta 295, 237–264.

Horibe, Y., Craig, H., 1995. DH fractionation in the system methane-hydrogen-water. Geochim. Cosmochim. Acta 59 (24), 5209–5217.

Horita, J., 1988. Hydrogen isotope analysis of natural waters using an H2-water equilibration method: a special implication to brines. Chemical Geology: Isotope Geoscience Section 72 (1), 89–94.

Horita, J., Wesolowski, D.J., 1994. Liquid-vapor fractionation of oxygen and hydrogen isotopes of water from the freezing to the critical temperature. Geochim. Cosmochim. Acta 58 (16), 3425–3437.

Kawagucci, S., Toki, T., Ishibashi, J., Takai, K., Ito, M., Oomori, T., Gamo, T., 2010. Isotopic variation of molecular hydrogen in 20–375 C hydrothermal fluids as detected by a new analytical method. J. Geophys. Res. Biogeo. 115 (G3).

Kirshenbaum, I., Urey, H. C., & Murphy, G. M. (1951). Physical properties and analysis of heavy water. National Nuclear Energy Series, McGraw–Hill, New York, 1951.

Lin, L.H., Slater, G.F., Lollar, B.S., Lacrampe-Couloume, G., Onstott, T.C., 2005. The yield and isotopic composition of radiolytic H2, a potential energy source for the deep subsurface biosphere. Geochim. Cosmochim. Acta 69 (4), 893–903.

Lord, A. S. (2009). Overview of geologic storage of natural gas with an emphasis on assessing the feasibility of storing hydrogen (No. SAND2009-5878). Sandia National Laboratories (SNL), Albuquerque, NM, and Livermore, CA (United States).

Lord, A.S., Kobos, P.H., Borns, D.J., 2014. Geologic storage of hydrogen: Scaling up to meet city transportation demands. Int. J. Hydrogen Energy 39 (28), 15570–15582.

Mangenot, X., Xie, H., Crémière, A., Giunta, T., Lilley, M., Sissmann, O., Eiler, J., 2023. 2H-2H clumping in molecular hydrogen method and preliminary results. Chem. Geol. 621, 121278.

Milkov, A.V., 2022. Molecular hydrogen in surface and subsurface natural gases: Abundance, origins and ideas for deliberate exploration. Earth Sci. Rev. 230, 104063.

Ohba, T., Hirabayashi, J.I., 1996. Handling of Pt catalyst in H2-H2O equilibration method for D/H measurement of water. Geochem. J. 30 (6), 373–377.

O'Neil, J.R., 1986. Theoretical and experimental aspects of isotopic fractionation. Rev. Mineral. 16, 1–40.

Pester, N.J., Conrad, M.E., Knauss, K.G., DePaolo, D.J., 2018. Kinetics of D/H isotope fractionation between molecular hydrogen and water. Geochim. Cosmochim. Acta 242, 191–212.

Popa, M.E., Paul, D., Janssen, C., Röckmann, T., 2019. H2 clumped isotope measurements at natural isotopic abundances. Rapid Commun. Mass Spectrom. 33 (3), 239–251.

Prinzhofer, A., Cissé, C.S.T., Diallo, A.B., 2018. Discovery of a large accumulation of natural hydrogen in Bourakebougou (Mali). Int. J. Hydrogen Energy 43 (42), 19315–19326.

Prinzhofer, A., Moretti, I., Françolin, J., Pacheco, C., d'Agostino, A., Werly, J., Rupin, F., 2019. Natural hydrogen continuous emission from sedimentary basins: The example of a Brazilian H2-emitting structure. Int. J. Hydrogen Energy 44 (12), 5676–5685.

Proskurowski, G., Lilley, M.D., Kelley, D.S., Olson, E.J., 2006. Low temperature volatile production at the Lost City Hydrothermal Field, evidence from a hydrogen stable isotope geothermometer. Chem. Geol. 229 (4), 331–343.

Rahn, T., Eiler, J.M., Boering, K.A., Wennberg, P.O., McCarthy, M.C., Tyler, S., Atlas, E., 2003. Extreme deuterium enrichment in stratospheric hydrogen and the global atmospheric budget of H2. Nature 424 (6951), 918–921.

Richet, P., Bottinga, Y., Janoy, M., 1977. A review of hydrogen, carbon, nitrogen, oxygen, sulphur, and chlorine stable isotope enrichment among gaseous molecules. Annu. Rev. Earth Planet. Sci. 5, 65–110.

Ricci, A., Kleine, B.I., Fiebig, J., Gunnarsson-Robin, J., Kamunya, K.M., Mountain, B., Stefánsson, A., 2022. Equilibrium and kinetic controls on molecular hydrogen abundance and hydrogen isotope fractionation in hydrothermal fluids. Earth Planet. Sci. Lett. 579, 117338.

Rolston, J.H., Den Hartog, J., Butler, J.P., 1976. The deuterium isotope separation factor between hydrogen and liquid water. J. Phys. Chem. 80 (10), 1064–1067.

Sherwood Lollar, B., Voglesonger, K., Lin, L.H., Lacrampe-Couloume, G., Telling, J., Abrajano, T.A., Pratt, L.M., 2007. Hydrogeologic controls on episodic H2 release from Precambrian fractured rocks—energy for deep subsurface life on Earth and Mars. Astrobiology 7 (6), 971–986.

Sherwood Lollar, B., Onstott, T.C., Lacrampe-Couloume, G., Ballentine, C.J., 2014. The contribution of the Precambrian continental lithosphere to global H2 production. Nature 516 (7531), 379–382.

Suda, K., Ueno, Y., Yoshizaki, M., Nakamura, H., Kurokawa, K., Nishiyama, E., Maruyama, S., 2014. Origin of methane in serpentinite-hosted hydrothermal systems: The CH4–H2–H2O hydrogen isotope systematics of the Hakuba Happo hot spring. Earth Planet. Sci. Lett. 386, 112–125.

Suess, H.E., 1949. Das Gleichgewicht H2+ HDO ⇌ HD+ H2 O und die weiteren Austauschgleichgewichte im System H2, D2 und H2O. Zeitschrift Für Naturforschung A 4 (5), 328–332.

Taiwo, G.O., Tomomewo, O.S., Oni, B.A., 2024. A comprehensive review of underground hydrogen storage: Insight into geological sites (mechanisms), economics, barriers, and future outlook. J. Storage Mater. 90, 111844.

Tarkowski, R., 2019. Underground hydrogen storage: Characteristics and prospects. Renew. Sustain. Energy Rev. 105, 86–94.

Truche, L., Donzé, F.V., Goskolli, E., Muceku, B., Loisy, C., Monnin, C., Cerepi, A., 2024. A deep reservoir for hydrogen drives intense degassing in the Bulqizë ophiolite. Science 383 (6683), 618–621.

Turner, A.C., Korol, R., Eldridge, D.L., Bill, M., Conrad, M.E., Miller III, T.F., Stolper, D. A., 2021. Experimental and theoretical determinations of hydrogen isotopic equilibrium in the system CH4H2H2O from 3 to 200° C. Geochim. Cosmochim. Acta 314, 223–269.

Urey, H.C., 1947. The thermodynamic properties of isotopic substances. Journal of the Chemical Society (resumed) 562–581.

Wang, D.T., Gruen, D.S., Lollar, B.S., Hinrichs, K.U., Stewart, L.C., Holden, J.F., Ono, S., 2015. Nonequilibrium clumped isotope signals in microbial methane. Science 348 (6233), 428–431.

Wang, D.T., Reeves, E.P., McDermott, J.M., Seewald, J.S., Ono, S., 2018. Clumped isotopologue constraints on the origin of methane at seafloor hot springs. Geochim. Cosmochim. Acta 223, 141–158.

Zgonnik, V., 2020. The occurrence and geoscience of natural hydrogen: A comprehensive review. Earth Sci. Rev. 203, 103140.

Zivar, D., Kumar, S., Foroozesh, J., 2021. Underground hydrogen storage: A comprehensive review. Int. J. Hydrogen Energy 46 (45), 23436–23462.